Evolution of Localized Damage Zone in Heterogeneous Media

SHENG-WANG HAO,[1,4] MENG-FEN XIA,[2,3] FU-JIU KE[1,2] AND YI-LONG BAI[2,*]

[1]*Department of Applied Physics, Beihang University Beijing 100083, China*

[2]*State Key Laboratory of Nonlinear Mechanics, Institute of Mechanics, Chinese Academy of Sciences, Beijing 100190, China*

[3]*Department of Physics, Peking University, Beijing 100871, China*

[4]*School of Civil Engineering and Mechanics, Yanshan University Qinhuangdao 066004, China*

ABSTRACT: Evolution of localized damage zone is a key to catastrophic rupture in heterogeneous materials. In the present article, the evolutions of strain fields of rock specimens are investigated experimentally. The observed evolution of fluctuations and autocorrelations of strain fields under uniaxial compression demonstrates that the localization of deformation always appears ahead of catastrophic rupture. In particular, the localization evolves pronouncedly with increasing deformation in the rock experiments. By means of the definition of the zone with high strain rate and likely damage localization, it is found that the size of the localized zone decreases from the sample size at peak load to an eventual value. Actually, the deformation field beyond peak load is bound to suffer bifurcation, namely an elastic unloading part and a continuing but localized damage part will co-exist in series in a specimen. To describe this continuous bifurcation and localization process observed in experiments, a model on continuum mechanics is developed. The model can explain why the decreasing width of localized zone can lead stable deformation to unstable, but it still has not provided the complete equations governing the evolution of the localized zone.

KEY WORDS: localized zone, catastrophic rupture, heterogeneous material.

*Author to whom correspondence should be addressed. E-mail: baiyl@lnm.imech.ac.cn

1056-7895/10/07 0787–18 $10.00/0 DOI: 10.1177/1056789509359660

INTRODUCTION

THE RUPTURE OF heterogeneous material like concrete, rock, and other materials is always accompanied by the localization of deformation and damage in a narrow zone (Rudnicki and Rice, 1975; Scarpelli and Wood, 1982; Loret and Prevost, 1990; Labuz and Biolzi, 1991; Poirier et al., 1992; Harris et al., 1995; Tordesillas, 2004; Wallin et al., 2008; Chow and Jie, 2009; Van and Man, 2009). This implies that when eventual rupture occurs the scale governing the rupture is much smaller than the sample size. Therefore, after localization, the response of a sample evolves from global to local (Labuz and Biolzi, 1991; Hao et al., 2007). Especially this results in the uncertainty of catastrophic rupture, because of the unknown size of the localized zone (Hao et al., 2007).

Experiments have revealed that the localized zone at rupture has narrow but finite widths (Scarpelli and Wood, 1982; Loret and Prevost, 1990; Labuz and Biolzi, 1991; Tordesillas, 2004; Hao et al., 2007). Hao et al. (2007) found that the final localized zones are about 6–8 mm, or almost 1/4 of specimen's size in their rock experiments and Lockner et al. (1991) reported an experimentally evaluated width of 2–5 mm. So, any analysis of macroscopic behavior excluding localization would be deficient. In addition, previous experiments have also revealed that the localized zone width may be strongly dependent on microscopic structure. For example Harris et al. (1995) reported that the width of localized zone can be up to 17 times of the average particle diameter, and around 10 particle diameters reported by Scarpelli and Wood (1982) and Roscoe (1970), 3–4 particle diameters reported by Calvetti et al. (1997). Moreover, the localized zones are also influenced by particle strength and the strength of interface between particles. It is reported (Tapponnier and Brace, 1976; Aydin and Johnson, 1978) that the crushing of individual grains and the transgranular cracks will appear during the formation of localized zone. These factors lead to even more complicated nucleation and evolution of localized zone. Hence, how the localized zone nucleates and grows remains an enigma.

On the other hand, the evolution of localized patterns is critical to the forecast of catastrophic rupture and the understanding of the failure mechanism of heterogeneous materials (Labuz and Biolzi, 1991; Hao et al., 2007). For instance, it is found that catastrophic rupture may be foreseen with acceptable error of 6% based on elastic and statistical brittle model (ESB), provided the width of localized zone is available (Bai and Hao, 2007). So, to determine the width of the localized zone and its evolution law becomes an unavoidable task in damage mechanics.

In the present article, a combined experimental and analytical study of the evolution of localized deformation zone is reported. To understand the

evolution of the localized zone observed in experiments, a model based on continuum mechanics is given. In order to capture the characteristics of the localized zone and its evolution, we firstly introduce the experimentally observed fluctuation and autocorrelation of strain fields of rock specimens under uniaxial compression, and then turn to the observation of the evolution and the analysis of the evolution of the localized zone.

EXPERIMENTAL OBSERVATIONS OF LOCALIZED DEFORMATION ZONE

In order to unveil the characteristics of the evolution of localized zone, the temporal evolution of fluctuations and the spatial autocorrelations of strains field of rock specimens were investigated under uniaxial compression, with the digital speckle correlation method (DSCM). The testing machine is servo-controlled and the specimens with dimensions of $20 \times 16 \times 40\,\text{mm}^3$ were loaded at a constant rate of 0.02 mm/min. The DSCM was coordinated with the loading system in order to detect the localization of deformation (Hao et al., 2007). The detailed testing process is described in the previous paper (Hao et al., 2007).

The fluctuations of strain are calculated to describe the evolution of non-uniform strain field. The relevant calculations are as follows:

(1) Mesh the sample surface with different window size d, and then move the window step by step and calculate the average strain $\varepsilon_J = 1/N \sum_{i=1}^{N(\text{calculating window})} \varepsilon_i$, where ε_i is the strain of the i-point in a window, N is the total of points in the window and subscript J represents the serial number of the windows, respectively.
(2) Calculate the fluctuation:

$$\text{Fluctuation}(d) = \frac{1}{n}\sum_{J=1}^{n}(\varepsilon_J - \langle\varepsilon\rangle)^2, \tag{1}$$

for a certain window size d, where $\langle\varepsilon\rangle$ is the average on the whole sample surface and n is the total of the windows, respectively.

(3) Calculate the fluctuations for different window size d.
(4) Calculate the fluctuations at different loading time.

On the other hand, we adopted Moran's I index (Moran, 1948; Getis and Ord, 1992) as a measure of the spatial autocorrelation of strain fields.

The greater the index I is the more closely the spatial autocorrelation. The index, represented by I, is calculated with:

$$I = \frac{n}{\sum_{i=1}^{n}\sum_{j=1}^{n} W_{ij}} \times \frac{\sum_{i=1}^{n}\sum_{j=1}^{n} W_{ij}(\varepsilon_i - \langle\varepsilon\rangle)(\varepsilon_j - \langle\varepsilon\rangle)}{\sum_{i=1}^{n}(\varepsilon_i - \langle\varepsilon\rangle)^2}, \tag{2}$$

where W_{ij} is a weight matrix, for which $W_{ij}=1$ if element i is connected to element j, otherwise $W_{ij}=0$.

To give a better evaluation of the spatial autocorrelation, we calculate the values of Moran's I at different window size d as follows:

$$I(d) = \frac{n}{\sum_{i=1}^{n}\sum_{j=1}^{n} W_{ij}(d)} \times \frac{\sum_{i=1}^{n}\sum_{j=1}^{n} W_{ij}(d)(\varepsilon_i - \langle\varepsilon\rangle)(\varepsilon_j - \langle\varepsilon\rangle)}{\sum_{i=1}^{n}(\varepsilon_i - \langle\varepsilon\rangle)^2}, \tag{3}$$

where $W_{ij}(d)=1$ when the distance between the elements i and j are equal or less than d, otherwise $W_{ij}(d)=0$. From Equation (3), we can see if ε_i and ε_j deviate from the average strain $\langle\varepsilon\rangle$ in the same way, their contribution to the index $I(d)$ is positive. Otherwise their contribution to Moran's I is negative. So, the larger the Moran's I is, the higher spatial autocorrelation the strain fields have.

The temporal evolution and the spatial autocorrelation of fluctuations in seven samples are investigated, among which two sample's results are shown in Figures 1–4, where time $t=0$ is set at the occurrence of eventual rupture, so the negative values denote the time lag ahead of the rupture. It can be seen that the autocorrelation of strains increase with the increasing fluctuations. This indicates that, with further deformation, the strain nonuniformity and the autocorrelation of strains are enhanced correspondingly. Especially,when rupture is approaching, the fluctuations and autocorrelations of all windows increase. This implicates that some high strain fields emerge and the localization of deformation appears ahead of the eventual macroscopic rupture. It should be noted that the strain fluctuations and the strain spatial autocorrelations in all samples increase with the decreasing window size, namely there is just a slight increase in the fluctuations for large windows; however, monotonically sharp increase is observed with smaller windows. And the more close to eventual rupture, the more obvious this tendency is. These indicate that the localized zone width may evolve from large to small. In order to obtain a more clear knowledge about the evolution of the localized zone, in the next section, we will examine the

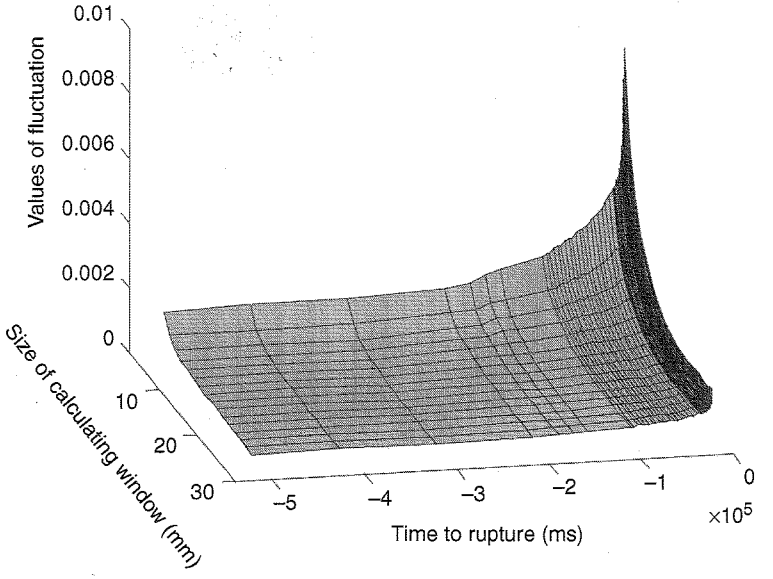

Figure 1. *The evolution of strain fluctuations of sample 1.*

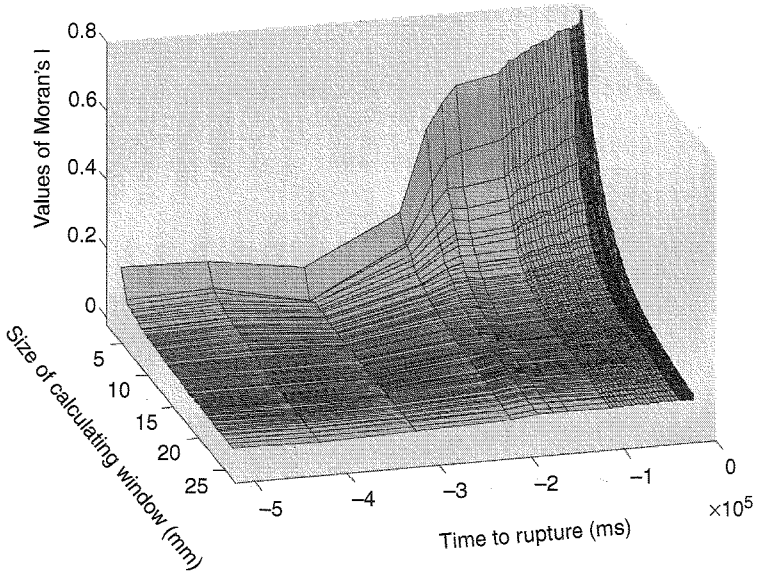

Figure 2. *The evolution of strain autocorrelation of sample 1.*

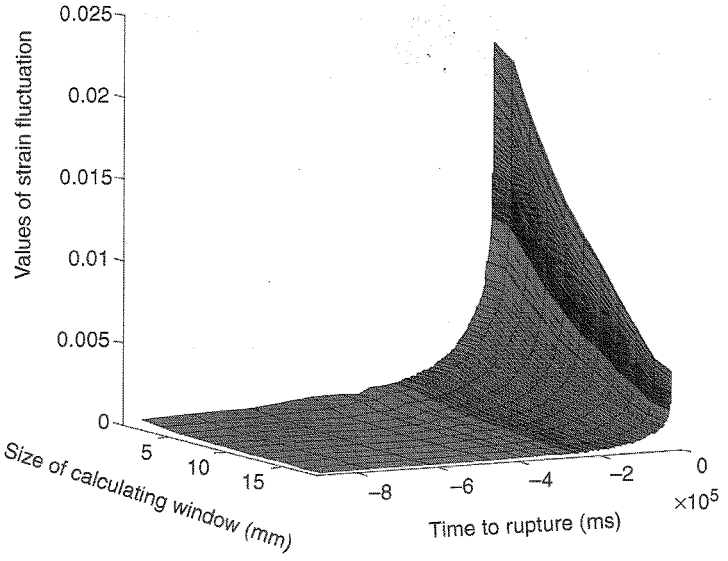

Figure 3. *The evolution of strain fluctuations of sample 2.*

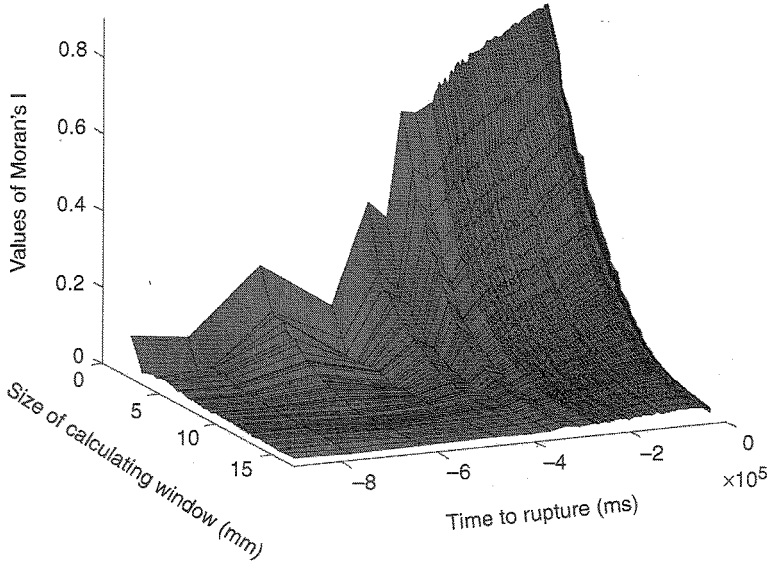

Figure 4. *The evolution of strain autocorrelation of sample 2.*

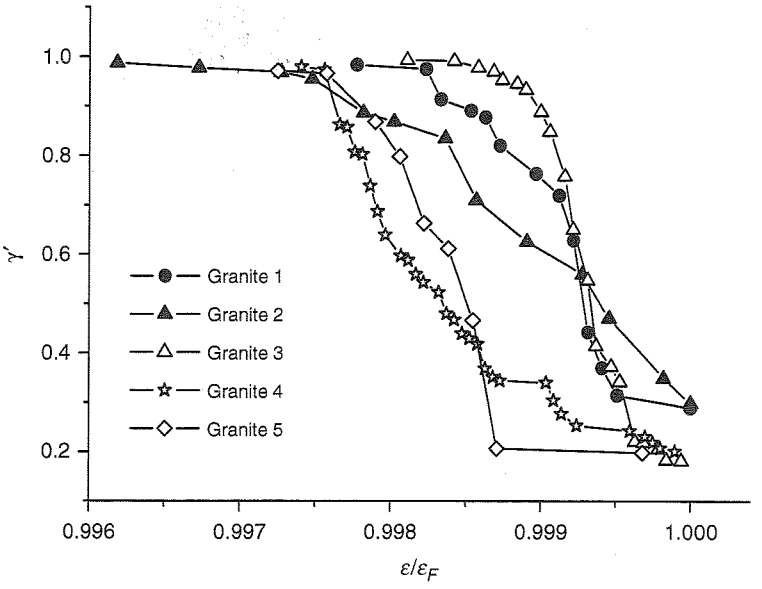

Figure 5. *The evolution of the zone with high strain rate and likely damage localization in granite samples.*

evolution of the zone with high damage rate in terms of experimental observation of rock's surface strain field evolution.

EVOLUTION OF THE ZONE WITH HIGH STRAIN RATE OF ROCK UNDER UNIAXIAL COMPRESSION

It is clear that the significant strain localization develops ahead of the rupture of rock specimens under uniaxial compression. So, there must be a close relation between the localization of damage and deformation. Now, we propose that the region where the strain rate remains less than the mean strain rate would not form the localized zone by any means. That is to say, the zone with high strain rate and likely damage localization can be defined as follows:

$$\frac{\mathrm{d}(\varepsilon_i - \langle\varepsilon\rangle)}{\mathrm{d}t} > 0 \text{ is satisfied at time } t \text{ and afterwards.}$$

According to this condition, the evolution of the zones with high strain rate and likely damage localization are calculated based on our experimental data and shown in Figures 5 and 6, where the size of the zone γ' is

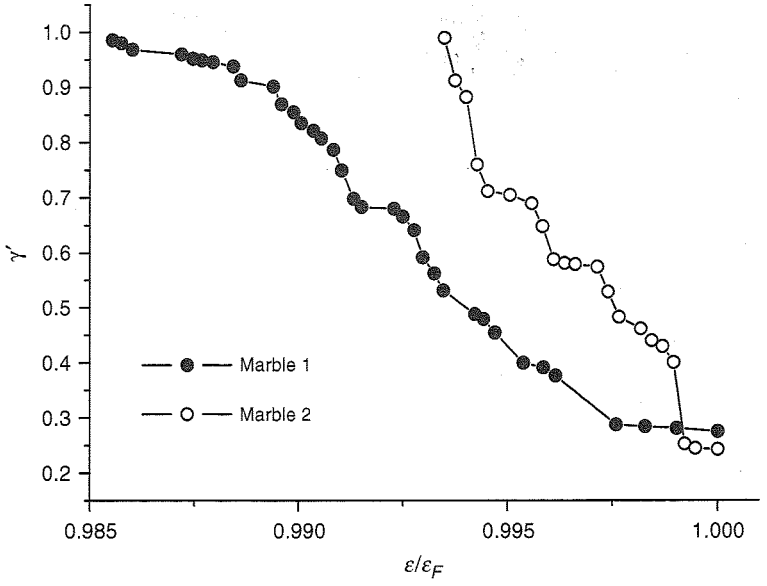

Figure 6. *The evolution of the zone with high strain rate and likely damage localization in marble samples.*

normalized with the size of the specimen, and the nominal strain ε is normalized with the rupture strain ε_F.

It can be seen that the scale γ' evolves from unit to an ultimate size, which almost equals to the ultimate width of the localized zone determined by the method in (Hao et al., 2007). This phenomenon is to be kept in mind, an analysis of the evolution of the localized zone will be given in the next section.

CONTINUOUS BIFURCATION AND LOCALIZATION

It has been shown in last section that localization is bound to appear ahead of catastrophic rupture. However, so far, there is still no physical understanding of how the localized zone evolves. Here, we suggest a possible mechanism of localization that a new phenomenon – continuous bifurcation – emerges beyond peak load. That is, in the load-descending phase there are always two possible ways of deformation: continuing damage (with increasing deformation) and elastically unloading (with decreasing deformation), see Figure 7. More importantly, the bifurcation will keep going on without interruption with the descending load. In fact,

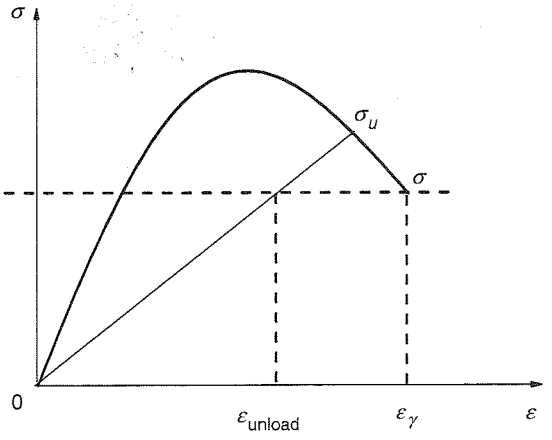

Figure 7. *A sketch of stress–strain relation of continuous bifurcation. At the current stress σ, the strain of the localized zone γ is ε_γ; whereas ε_{unload} marked in this figure represents only the strain of the stripe $d(1-\gamma(\sigma_u))$ in the unloading part $(1-\gamma)$.*

we have not had any knowledge of the partition of a macroscopic sample into the two parts during the continuous bifurcation yet.

In this section, based on the conservation laws of continuum mechanics and the ESB model (for the details of ESB model under global mean field approximation, please see Appendix), we intend to gain an insight into the continuous bifurcation and the evolution of the localized zone. In order to do this, we consider a stiff loading condition and take the following local mean field assumptions (Figure 8):

(1) Continuous bifurcation and damage localization appears and evolves beyond the peak load in a macroscopic sample, see Figure 7.
(2) As soon as damage localization appears, the sample can be regarded as two parts in series, namely a continuing damage zone and an elastically unloading zone under the same nominal stress, see Figures 7 and 8.
(3) Mean field approximation works for each zone, see Figure 8. Additionally, the linear dimension of the localized zone is denoted by $0 \leq \gamma \leq 1$, whilst the unloading zone is $1-\gamma$, Figure 8. Together with assumption 1, at the peak load σ_M, $\gamma = 1$.
(4) During the loading process, either the whole sample before the peak load or the part γ beyond the peak load follows the same ESB relation $\sigma = f(\varepsilon)$, see Figure 7.
(5) The unloading in the part $(1-\gamma)$ is assumed to be linearly elastic with no residual strain in the ESB model, namely $\sigma_u - \sigma = E_u(\sigma_u)(\varepsilon_u - \varepsilon)$, where E_u is the unloading elastic constant and σ_u and ε_u denote the

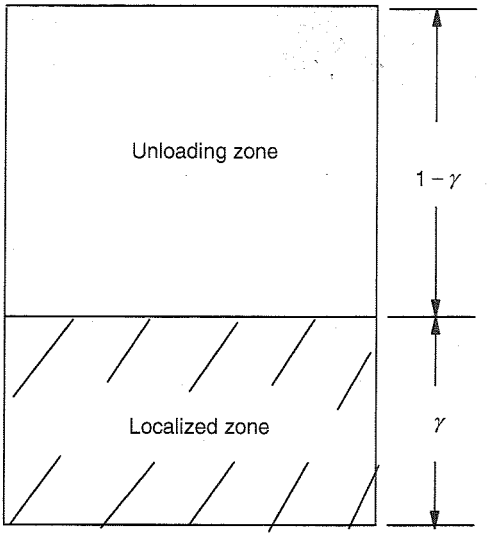

Figure 8. *A sketch of local mean field approximation.*

state, where the unloading starts, see Figure 7. Actually, the unloading part $(1-\gamma)$ is by no means uniform as the part γ, because the unloading part $1-\gamma$ consists of a series of small parts with different strain $\varepsilon_{\text{unload}} = \varepsilon_{\text{unload}}(\sigma, \sigma_u, \varepsilon_u)$ resulting from elastic unloading with different starting states $(\sigma_u, \varepsilon_u)$, see Figure 7.

According to the force balance law, the normal stress in both zones in the series is equal to the nominal stress σ. Also, because there are different strain increments in the two zones under the same stress decrement in the load-descending phase, we will take the nominal stress σ as the independent variable later. Then, in accord with assumption 4, the strain of the localized zone γ is:

$$\varepsilon_\gamma(\sigma) = f^{-1}(\sigma) = \frac{\sigma}{E_u(\sigma)},$$

and the tangential modulus of the localized zone $E_\gamma(\sigma)$ satisfies:

$$\begin{aligned} \frac{\mathrm{d}\varepsilon_\gamma}{\mathrm{d}\sigma} &= \frac{1}{E_\gamma(\sigma)} \\ &= \frac{\mathrm{d}}{\mathrm{d}\sigma}\left(\frac{\sigma}{E_u(\sigma)}\right) = \frac{1}{E_u(\sigma)} - \frac{\sigma}{E_u^2(\sigma)} E_u'(\sigma). \end{aligned} \tag{4}$$

Now, let us examine the effect of continuous bifurcation on deformation. Owing to the continuous bifurcation, the nominal stain of the unloading zone $(1-\gamma)$ at stress σ, that is, $\varepsilon_{1-\gamma}(\sigma)$, should be the accumulation of the deformations from various unloading stress σ_u in the unloading zone $(1-\gamma)$ as:

$$\begin{aligned}\varepsilon_{1-\gamma}(\sigma)(1-\gamma(\sigma)) &= \int_{\sigma_M}^{\sigma} \varepsilon_{\text{unload}}(\sigma,\sigma_u)\mathrm{d}(1-\gamma(\sigma_u)) = \int_{\sigma_M}^{\sigma} \frac{\sigma}{E_u(\sigma_u)}\mathrm{d}(1-\gamma(\sigma_u)) \\ &= \frac{\sigma}{E_u(\sigma)}(1-\gamma(\sigma)) + \int_{\sigma_M}^{\sigma} \frac{\sigma(1-\gamma(\sigma_u))E_u'(\sigma_u)}{E_u^2(\sigma_u)}\mathrm{d}\sigma_u. \end{aligned} \tag{5}$$

Hence, the deformation rate of the unloading zone with respect to the nominal stress σ can be expressed as:

$$\begin{aligned}\mathrm{d}[\varepsilon_{1-\gamma}(\sigma)(1-\gamma(\sigma))]/\mathrm{d}\sigma &= \frac{1}{E_u(\sigma)}(1-\gamma(\sigma)) - \frac{\sigma}{E_u(\sigma)}\gamma'(\sigma) \\ &\quad + \int_{\sigma_M}^{\sigma} \frac{(1-\gamma(\sigma_u))E_u'(\sigma_u)}{E_u^2(\sigma_u)}\mathrm{d}\sigma_u. \end{aligned} \tag{6}$$

In accord with continuity law, the total strain of the macroscopic sample should be the weighted sum of the strains of the two zones as:

$$\begin{aligned}\varepsilon_{\text{total}} &= \varepsilon_\gamma \cdot \gamma + \varepsilon_{1-\gamma} \cdot (1-\gamma) \\ &= \frac{\sigma}{E_u(\sigma)} \cdot \gamma(\sigma) + \frac{\sigma}{E_u(\sigma)}(1-\gamma(\sigma)) + \int_{\sigma_M}^{\sigma} \frac{\sigma(1-\gamma(\sigma_u))E_u'(\sigma_u)}{E_u^2(\sigma_u)}\mathrm{d}\sigma_u. \end{aligned}$$

Obviously, only if the evolution law $\gamma(\sigma)$ is available, the nominal stress–strain relation $\sigma(\varepsilon_{\text{total}})$ can be calculated accordingly. Clearly, the evolution law $\gamma(\sigma)$ cannot be deduced from the above equation based on continuity and force balance laws. So, we have to resort to energy conservation to see if we can obtain the evolution law of the localized zone $\gamma(\sigma)$.

The total of the work increment on the macroscopic sample with respect to the nominal stress σ should be:

$$\begin{aligned}\mathrm{d}W/\mathrm{d}\sigma &= \sigma\mathrm{d}\varepsilon_{\text{total}}/\mathrm{d}\sigma = \sigma\mathrm{d}[\varepsilon_\gamma \cdot \gamma + \varepsilon_{1-\gamma} \cdot (1-\gamma)]/\mathrm{d}\sigma \\ &= \sigma\mathrm{d}[\sigma/E_u(\sigma) \cdot \gamma(\sigma)]/\mathrm{d}\sigma + \sigma\mathrm{d}[\varepsilon_{1-\gamma}(\sigma) \cdot (1-\gamma(\sigma))]/\mathrm{d}\sigma. \end{aligned} \tag{7}$$

In addition, $\mathrm{d}W/\mathrm{d}\sigma$ is equal to 0 when catastrophic rupture occurs. Substituting Equation (6) into Equation (7), we can obtain

$$-\frac{\mathrm{d}W}{\mathrm{d}\sigma} = \frac{\sigma^2\gamma(\sigma)}{E_u^2(\sigma)}E_u'(\sigma) + \int_{\sigma_M}^{\sigma} \frac{\sigma\gamma(\sigma_u)}{E_u^2(\sigma_u)}E_u'(\sigma_u)\mathrm{d}\sigma_u - \frac{\sigma}{E_u(\sigma_M)}. \tag{8}$$

Equation (8) is a certain relation between work increment (note $-dW/d\sigma > 0$ in the load-descending phase) and the size of localized zone $\gamma(\sigma)$. Now, there are some points worth noting.

(1) Although an integral is involved owing to continuous bifurcation, this remains a linear dependence of the work increment on localized zone $\gamma(\sigma)$, due to the extensive nature of deformation.
(2) Since the work increment $-dW/d\sigma > 0$ indicates stable deformation and $dW/d\sigma = 0$ indicates catastrophic rupture, as well as differentiation $E_u'(\sigma_u) > 0$ in the load-descending phase, the smaller the localized zone γ in the first two terms is, the more likely the deformation to become unstable. This is what the experimental observation shows: damage localization leads to catastrophic failure.

Now, in order to determine the evolution of the localized zone γ (σ), we must know the work increment independently. Unfortunately, it is found that the energy increment has exactly the same expression of the work increment, namely energy conservation law leads to an identical equation for any value of γ (σ). In one word, we cannot determine the evolution of the localized zone γ (σ), in the light of energy conservation. Therefore, we must go beyond the continuum mechanics, to seek the mechanism governing the continuous bifurcation and the evolution of localized zone.

DISCUSSIONS

The experimental observations of rock tests under uniaxial compression show that with increasing deformation both fluctuations and autocorrelations of strain field increase obviously beyond peak load. Afterwards, deformation concentrates in a narrow zone leading to eventual rupture. By means of the definition of the zone with high strain rate and likely damage localization, $(d(\varepsilon_i - \langle\varepsilon\rangle)/dt) > 0$ is satisfied at time t and afterwards, the evolution of the localized zone γ is investigated in rock experiments. In both granite and marble, the size of the localized zone γ decreases from the sample size, that is, $\gamma = 1$, at peak load to an eventual value.

Based on the observations of the bifurcation of deformation beyond peak load, a model based on continuous bifurcation is developed. In this model, a sample will split into an elastically unloading part and a continuing but localized damage part in series. Although the continuum model is still not enough to determine the width of the localized damage zone definitely, it reveals how the decreasing width of localized zone leads to the transition from stable to unstable deformation in the sample.

Since the width of localized damage zone is critical to both post-peak behavior and catastrophic rupture of heterogeneous materials, the establishment of a proper model to depict the evolution of localized damage zone is a real challenge to damage mechanics.

ACKNOWLEDGMENTS

This work is supported by the National Natural Science Foundation of China (Grant Nos. 90715001, 10721202, 10572139, 10972218 and 10802073), the National Basic Research Program of China (973 Program 2007CB814800), and the CAS Innovation Program.

APPENDIX

Elastic and Statistically Brittle Constitutive Model

Elastic and statistically brittle (ESB) model is a trans-scale version of macroscopic constitutive relation for mesoscopically heterogeneous media, Figure A1.

Suppose that all intact mesoscopic units in the macroscopic sample follow the same linear elastic law:

$$\sigma_s = E_0 \varepsilon_s, \tag{A1}$$

where σ_s, ε_s, and E_0 are the true stress and strain of the meso-units and E_0 is the elastic constant, respectively, Figure A2. But, each mesoscopic unit has its own breaking threshold σ_c, namely as soon as the stress in the unit reaches its stress threshold σ_c, the unit will suffer brittle breaking and then it can no longer sustain any load, see Figure A2.

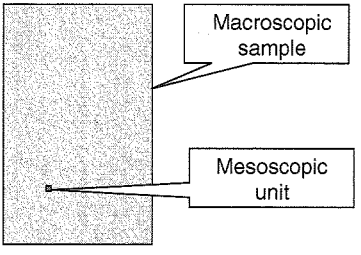

Figure A1. *A sketch of the trans-scale ESB model: a macroscopic sample consists of a number of mesoscopic heterogeneous units.*

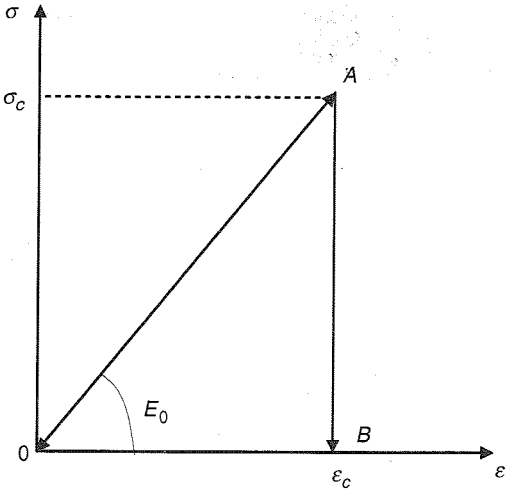

Figure A2. *The elastic and brittle constitutive relation of a mesoscopic unit. Below the stress threshold $\sigma_c = E_0\varepsilon_c$ (i.e., within OA), the mesoscopic unit is linear elastic (reversible). However, as soon the stress in the unit reaches its stress threshold σ_c, the unit will irreversibly break and its stress will drop to zero (point B).*

But the mesoscopic units in the macroscopic sample have different breaking thresholds σ_c, which follow a distribution function $h(\sigma_c)$, like Weibull distribution:

$$h(\sigma_c) = m\left(\frac{\sigma_c}{\eta}\right)^{m-1} \exp\left[-\left(\frac{\sigma_c}{\eta}\right)^{m}\right], \tag{A2}$$

where m and η are Weibull modulus and position parameter, respectively. Clearly, the position parameter η serves as the scale of the breaking thresholds σ_c, whereas Weibull modulus m indicates the heterogeneity of the mesoscopic breaking threshold σ_c.

Later, we will use the normalized stress and strain $\sigma = stress/\eta$ and $\varepsilon = (\text{strain}^* E_0)/\eta$ in our formulation of ESB model, hence the Weibull distribution (A2) can be expressed as:

$$h(\varepsilon_c) = m(\varepsilon_c)^{m-1}\exp[-(\varepsilon_c)^m], \tag{A2a}$$

where ε_c is the normalized strain threshold. Figure A3 shows how Weibull modulus m represents the heterogeneity of the breaking threshold ε_c.

If global mean field approximation was adopted as conventional damage mechanics do, all undamaged mesoscopic units would sustain the same true stress $\sigma_s = \sigma/(1-D)$ and strain $\varepsilon_s = \varepsilon$, where D is damage. On the other hand,

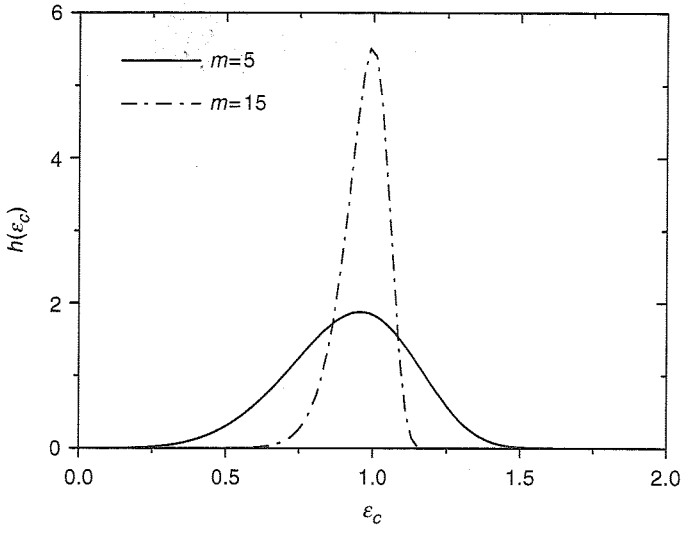

Figure A3. *Weibull distributions of the normalized strain threshold ε_c, Equation (A2a), for different Weibull modulus: $m=5$ (solid line) and $m=15$ (dashed line), showing that the greater the Weibull modulus is, the more homogenous the sample is. Also, the shaded area under the distribution curve is actually the damage $D(\varepsilon)$, according to Equation (A3).*

when a mesoscopic unit attains its breaking threshold σ_c, it cannot sustain load any more, hence damage D in the macroscopic sample can be expressed as:

$$D = \int_0^{\varepsilon_s} h(\varepsilon_c)\mathrm{d}\varepsilon_c = 1 - \exp(-\varepsilon^m), \tag{A3}$$

since the normalized strain of the macroscopic sample ε is equal to the true strain ε_s according to damage mechanics, see Figure A3.

Together with the basic relation in damage mechanics $\sigma = (1-D)\varepsilon$ for a macroscopic element, one can deduce the 1D ESB constitutive relation of σ, ε, and D as follows (also see Krajcinovic 1996):

$$\sigma = F(\varepsilon) = \varepsilon \exp(-\varepsilon^m), \tag{A4}$$

$$\sigma = G(D) = (1-D)[-\ln(1-D)]^{\frac{1}{m}}. \tag{A5}$$

For simplicity, suppose that unloading be linearly elastic with no residual strain, the corresponding unloading relation can be written as:

$$\sigma_u - \sigma = \varepsilon_u - \varepsilon, \tag{A6}$$

where the subscript u denotes the state, where the unloading starts.

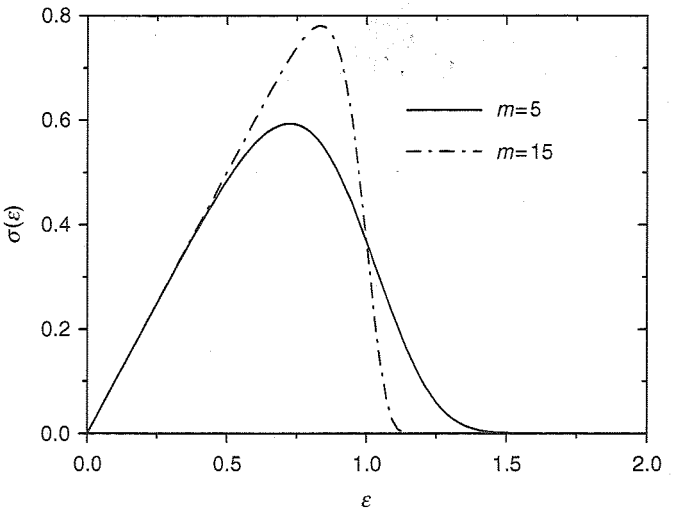

Figure A4. *The ESB constitutive relations for a macroscopic sample consisting of heterogeneous mesoscopic units, with Weibull distribution $m=5$ (solid line) and $m=15$ (dashed line), Equation (A4). The comparison of this figure and Figure A2 shows that the greater the Weibull modulus is, the more prone the macroscopic sample is to homogenous elastic-brittle.*

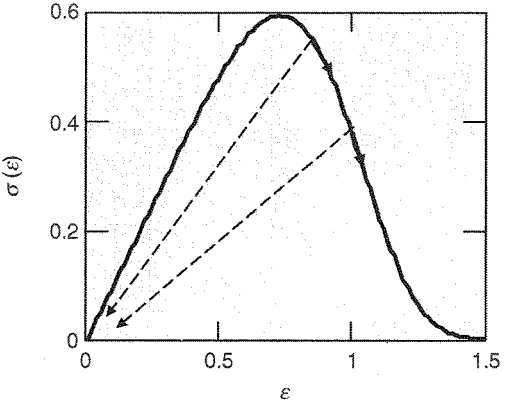

Figure A5. *The ESB constitutive relation ($m=5$) with elastic unloading, Equations (A4) and (A6). The bold solid line shows the variation of nominal stress with increasing strain, but the dashed lines show different elastic unloadings starting from different stress states.*

Above all, Equations (A4)–(A6) form a complete 1D constitutive relation of ESB model, see Figure A4. This implies that the ESB model can depict both phases of increasing and decreasing with one parameter only, that is, Weibull modulus m.

In addition, provided the mean field approximation always works, the relation of stress versus strain is unique in the load increasing phase, while in the load decreasing phase, the macroscopic sample can evolve either with increasing strain and further damage or with deceasing strain but elastic unloading along with fixed damage, see Figure A5.

REFERENCES

Aydin, A. and Johnson, A. (1978). Development of Faults as Deformation Bands in Porous Sandstones, *Pure and Applied Geophysics*, **116**: 931–942.

Bai, Y.L. and Hao, S.W. (2007). Elastic and Statistical Brittle (ESB) Model, Damage Localization and Catastrophic Rupture, In: Li, A., Sih, G., Nied, H. and Li, Z. (eds), *Proceedings of the International Conference on Health Monitoring of Structure, Material and Environment*, Nanjing, Southeast University Press, pp.1–5.

Calvetti, F., Combe, G. and Lanier, J. (1997). Experimental Micromechanical Analysis of a 2D Granular Material: Relation between Structure Evolution and Loading Path, *Mechanics of Cohesive-Frictional Materials*, **2**: 121–163.

Chow, C.L. and Jie, M. (2009). Anisotropic Damage-coupled Sheet Metal Forming Limit Analysis, *International Journal Of Damage Mechanics*, **18**: 371–392.

Getis, A. and Ord, J.K. (1992). The Analysis of Spatial Association by the Use of Distance Statistics, *Geographical Analysis*, **24**: 189–206.

Hao, S.W., Wang, H.Y., Xia, M.F., Ke, F.J. and Bai, Y.L. (2007). Relationship Between Strain Localization and Catastrophic Rupture, *Theoretical and Applied Fracture Mechanics*, **48**: 41–49.

Harris, W.W., Viggiani, G., Mooney, M.A. and Finno, R.J. (1995). Use of Stereophotogrammetry to Analyze the Development of Shear Bands in Sand, *Geotechnical Testing Journal*, **18**: 405–420.

Krajcinovic D. (1996). *Damage Mechanics*, North-Holland, Elsevier, Amsterdam, The Netherlands.

Labuz, J.F. and Biolzi, L. (1991). Class I vs Class II Stability: A Demonstration of Size Effect, *International Journal of Rock Mechanics and Mining Science*, **28**: 199–205.

Lockner, D.A., Byerlee, J.D., Kuksenko, V.A. and Ponomarev, A.S. (1991). Quasi-static Fault Growth and Shear Fracture Energy in Granite, *Nature*, **350**: 39–42.

Loret, B. and Prevost, J.H. (1990). Dynamic Strain Localization in Elasto-(visco-)plastic Solids, Part 2. Plane Strain Examples, *Computer Methods in Applied Mechanics and Engineering*, **83**: 247–273.

Moran, P. (1948). The Interpretation of Statistical Maps, *Journal of the Royal Statistical Society*, **10B**: 243–251.

Poirier, C., Ammi, M., Bideau, D. and Troadec, J.P. (1992). Shear Localization and Shear Instability in Materials in the Ductile Field, *Physical Review Letters*, **68**: 216–219.

Roscoe, K.H. (1970). The Influence of Strains in Soil Mechanics.10th Rankine Lecture, *Geotechnique*, **20**: 129–170.

Rudnicki, J.W. and Rice, J.R. (1975). Conditions for the Localization of Deformation in Pressure-sensitive Dilatant Materials, *Journal of the Mechanics and Physics of Solids*, **23**: 371–394.

Scarpelli, G. and Wood, D.M. (1982). Experimental Observations of Shear Band Patterns in Direct Shear Tests, In: *Proceedings of IUTAM Conference on Deformation and Failure of Granular Materials*, Delft, Rotterdam, Balkema Publ., pp. 473–484.

Tapponnier, P. and Brace, W.F. (1976). Development of Stress-induced Microcracks in Westerly Granite, *International Journal of Rock Mechanics and Mining Science*, **13**: 103–112.

Tordesillas, A., Peters, J.F. and Gardiner, B.S. (2004). Shear Band Evolution and Accumulated Microstructural Development in Cosserat Media, *International Journal for Numerical and Analytical Methods*, **28**: 981–1010.

Van Milder, J.G.M. and Man, H.K. (2009). Some Notes on Microcracking, Softening, Localization and Size Effects, *International Journal Of Damage Mechanics*, **18**: 283–309.

Wallin, M., Olssom, M. and Ristinmaa, M. (2008). Modeling of the Degradation of Elastic Properties due to the Evolution of Ductile Damage, *International Journal Of Damage Mechanics*, **17**: 149–172.